Invited paper presented at the "Thorium Energy Alliance 4th Annual 'Future of Energy' Conference," Loyola University, Water Tower Campus, Chicago, Illinois, USA, May 31 –June 1st 2012.

ELECTRODYNAMIC INERTIAL FUSION GENERATORS AND FISSION SATELLITES

Magdi Ragheb and Monish Singh

Department of Nuclear, Plasma and Radiological Engineering
University of Illinois at Urbana-Champaign,
216 Talbot Laboratory,
104 South Wright Street,
Urbana, Illinois 61801, USA.
https://netfiles.uiuc.edu/mragheb/www
mragheb@illinois.edu
msingh22@illinois.edu

ABSTRACT

The use of Diode and Wiffle Ball (WB) cusped magnetic field configurations is discussed in the context of their use as compact drivers in Electrostatic and Electrodynamic Inertial Confinement (EIC) Fusion, for a Fusion-Fission Hybrid using a thorium molten salt breeder.

The use of a fusion fission thorium hybrid in association with these configurations considering the catalyzed DD and the DT fusion reactions and a molten salt using Th^{232} as a U^{233} breeder is analyzed.

Energy and material balances in the coupled system as well as neutronic and photonic computations are conducted. They shows that the energy multiplication in the coupled system approaches infinity as the conversion ratio of the fission satellites approaches unity.

Such a configuration would allow enough energy breakeven for a sustainable long term energy system with a practically unlimited fuel supply base. Deuterium can be extracted from water in the world oceans, and thorium is four times more abundant than uranium in the Earth's crust.

The approach would provide the possibility for the eventual introduction of aneutronic fusion cycles such as the pB^{11} cycle for energy production as well as for space propulsion.

Such an alternative sustainable paradigm would provide the possibility of an optimized fusion-fission thorium hybrid for long term fuel availability with the added advantages of higher temperatures thermal efficiency for process heat production for a future hydrogen economy, proliferation resistance and minimized waste disposal characteristics.

INTRODUCTION

Cusped magnetic field configurations have been considered in fusion research in several contexts since they offer a situation where the confined plasma is stable against perturbations.

A linear cusped configuration was earlier proposed by Ragheb et al. in 1985 for the magnetic protection of the first wall of a DHe^3 low-tritium inventory fusion inertial confinement reactor using heavy ions as drivers [1, 2]. It protected the wall from the impingement of the charged particles and diverted them to collectors for direct energy conversion into electricity at a high conversion efficiency. The cusped configuration was modified, upon review, into an

alternative liquid metal fall for the protection of the first wall transforming the charged particles' kinetic energy into thermal energy. In this work, a low-tritium-inventory, high-power-density, pool-type chamber approach to inertial confinement fusion was introduced. The concept used target designs with internal tritium and He^3 breeding, eliminating the need for a lithium-breeding blanket. The fraction of the fusion energy carried out by neutrons is estimated as 10 percent, compared with 70 percent in a typical DT system, and the neutron spectrum was softer. Liquid metals other than lithium that are less chemically reactive, such as lead, could be used for first-wall protection. The reduced neutron component and the elimination of the need for a thick lithium blanket for tritium breeding lead to higher power densities and more compact chamber designs. The radiation damage at the first structural wall was reduced, leading to potentially longer wall lifetimes. A significant environmental advantage in terms of reduced radioactive release risks under operational and accidental conditions was identified, primarily due to the one to two orders of magnitude reduction in the tritium inventories compared with DT-based systems conceptual designs [1].

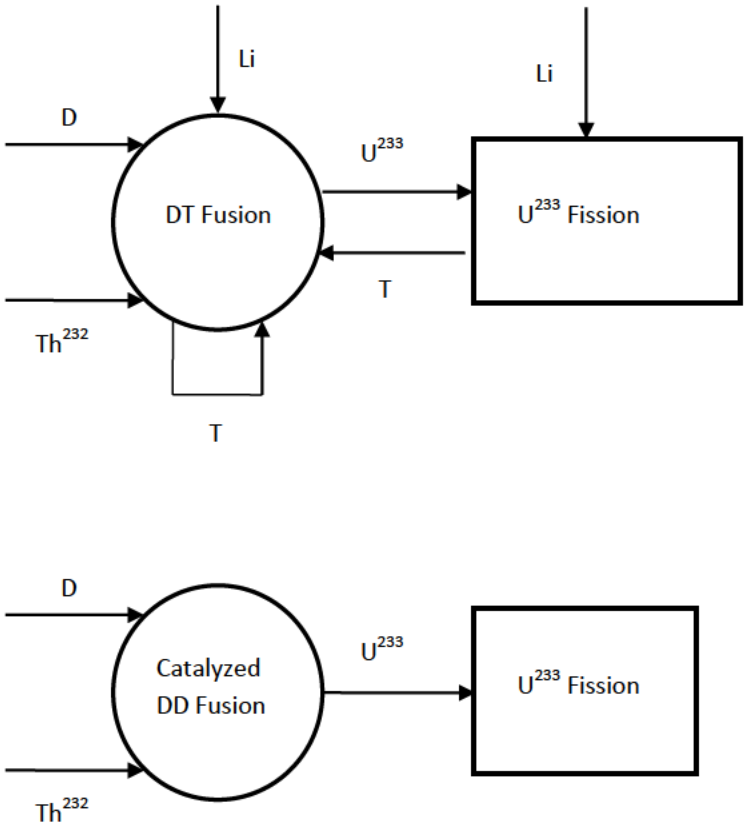

Figure 1. Material flows in the DT (top) and Catalyzed DD fusion-fission hybrid (bottom) alternatives with U^{233} breeding from Th^{232}.

A device using a quasi-spherical configuration was later introduced by Robert Bussard [3]. Starting in 1987 and published in 1991, Bussard [3] used the cusp configuration for inertial

electrodynamic fusion in a concept called the "Polywell" concept. The idea is to trap high densities of energetic electrons within a quasi-spherical magnetic field into which a current of high energy electrons is injected. The electrons form a deep negative potential well, without the need for mechanical grids. A small deviation from charge neutrality of 10^{-6} of ions versus electrons is required to make the potential well as deep as the electron drive energy [4]. The ions to be fused are then "dropped" at the edge of the created well. They fall into the center with an $1/r^2$ distribution of increasing density acquiring enough kinetic energy to make fusion reactions possible as they collide at the core region. Whenever scattering occurs, the ions recirculate back up the well and then fall in again when they reach the edge. Eventually, similar to the electrons, the ions' gyro motion in the increasing edge magnetic field of the system. The critical consideration is the power balance between the fusion power generation and the electron drive power loss. This depends on the ability of the magnetic field to keep the ions trapped in the quasi-sphere electron-driven electrostatic potential well. The fusion generation process and the electron trapping and losses are decoupled and can be optimized separately.

Table 1: Catalyzed DD and DT Fusion Reaction Energetics.

Reaction	Total Energy from fusion, E_f (MeV)	Charged Particle Energy (MeV)	Neutron Energy (MeV)	Fraction of energy to neutrons, f_n (%)	Number of Neutrons
DT reaction					
$_1D^2 + {}_1T^3 \rightarrow {}_2He^4(3.52) + {}_0n^1(14.06)$	17.57	3.52	14.06	80.02	1
Catalyzed DD reaction*					
(a) $\frac{1}{2}{}_1D^2 + \frac{1}{2}{}_1D^2 \rightarrow \frac{1}{2}{}_1T^3(1.01) + \frac{1}{2}{}_1H^1(3.03)$	4.04	4.04	0.00	0.00	0
(b) $\frac{1}{2}{}_1D^2 + \frac{1}{2}{}_1D^2 \rightarrow \frac{1}{2}{}_2He^3(0.82) + \frac{1}{2}{}_0n^1(2.45)$	3.66	2.43	1.23	33.61	1/2
(c) $\frac{1}{2}{}_1D^2 + \frac{1}{2}{}_1T^3 \rightarrow \frac{1}{2}{}_2He^4(3.52) + \frac{1}{2}{}_0n^1(14.06)$	8.79	1.76	7.03	80.02	1/2
(d) $\frac{1}{2}{}_1D^2 + \frac{1}{2}{}_2He^3 \rightarrow \frac{1}{2}{}_2He^4(3.67) + \frac{1}{2}{}_1H^1(14.67)$	9.17	9.17	0.00	0.00	0
----------	--------	---------	---------	--------	---
$3_1D^2 \rightarrow {}_2He^4 + {}_1H^1 + {}_0n^1$	21.62	13.36	8.26	38.21	1

*DD reactions (a) and (b) are assumed to have a branching ration of ½ and proceed at an equal rate: $R_1 = R_2 = \frac{R_{DD}}{2}$

DT and DHe^3 reactions (c) and (d) proceed at the same rate as the two DD reactions.

As initially suggested in 1987, coil conductors with zero cross sectional radius were placed exactly at the vertex edges with sharp corners where the coils came together. This leads to a "funny cusp" where an odd point/radial line appear sat such corners with a zero magnetic field at a zero radius.

SYMBIOTIC COUPLING OF FUSION BREEDERS AND FISSION SATELLITES, ENERGY AND MATERIAL BALANCES

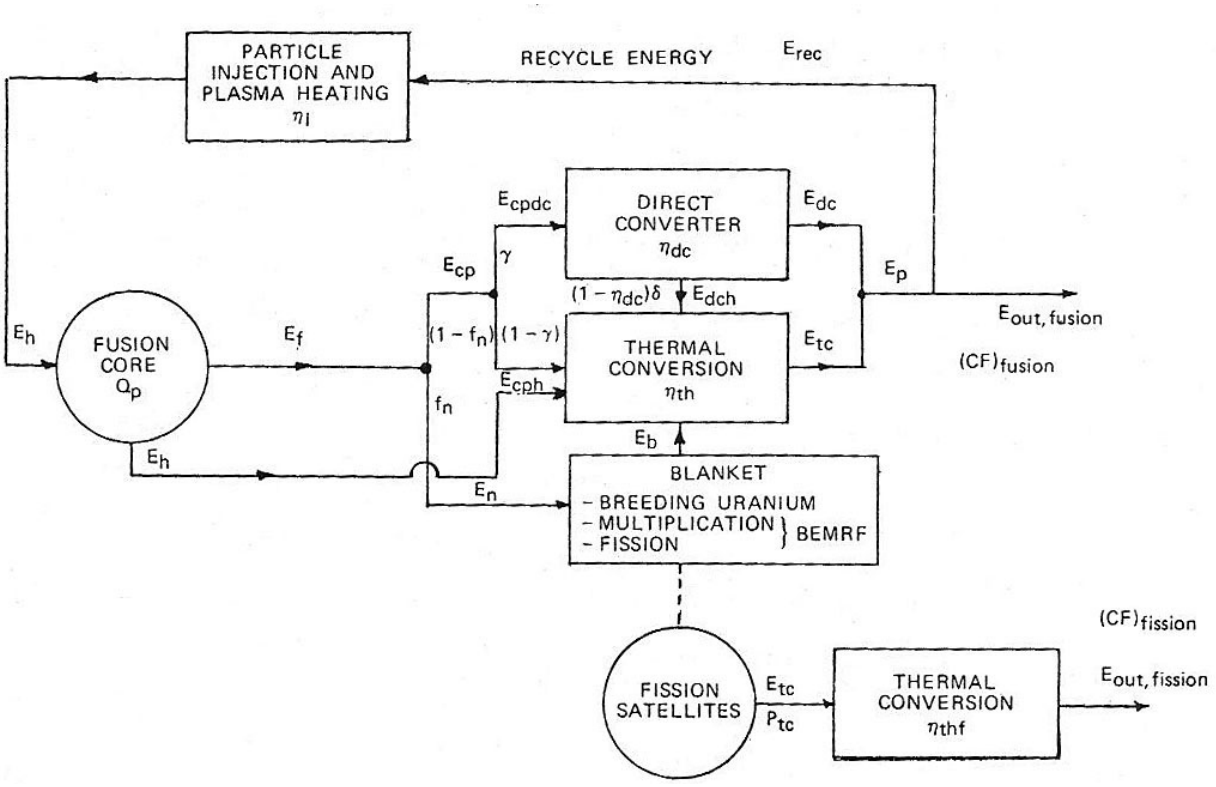

Figure 2. Energy and material flows in the symbiotic coupling of fusion breeder drivers and fission satellites.

The purpose of a symbiotic system is to provide fissile fuel bred in the fusion reactors for satellite fission burners of the fuel. Material and energy flows balances are necessary to optimize the coupling and identify the best configurations.

The "driven" system shown in Fig. 2 is considered. Let E_f be the fusion energy output per unit fusion reaction. One DT reaction releases a neutron having an energy of 14.06 MeV and the catalyzed DD reaction releases a neutron having an average energy of 8.26 MeV. From Table 1:

$$E_f(DT) = 17.57[\frac{MeV}{fusion}],$$

$$E_f(DD) = 21.62[\frac{MeV}{fusion}].$$

PLASMA POWER AMPLIFICATION FACTOR Q_p

An important design parameter for a magnetic fusion reactor is its plasma power amplification factor Q_p, defined as the ratio of the thermonuclear power produced to the power input to generate and heat the plasma to thermonuclear fusion temperatures:

$$Q_p = \frac{P_{thermonuclear}}{P_{input}} = \frac{E_f}{E_h} = \frac{\text{fusion energy generated in the plasma}}{\text{energy required to heat the plasma}} \qquad (1)$$

In a closed system, such as a toroidal Tokamak or Stellarator device, large values of Q_p are possible. Once the energy in the ions released from the fusion reactions in the plasma exceeds the radiation and other losses, plasma ignition should occur. The use of neutral ion beams injection or microwave radiofrequency heating can thus be stopped, and the plasma burn becomes self-sustained, as long as the fusion fuel continues being supplied, and the plasma remains confined.

In an open system such as a mirror or a cusped configuration fusion reactor, because of the inevitable end losses, it is unlikely that ignition can be achieved. Such devices would have to be used as a driven power amplifier. With a low value of Q_p, energy would have to be supplied continuously and the fusion reaction would amplify the energy input to the plasma by the factor Q_p. In a single-cell plasma, Q_p may not exceed about 1.2. The magnetic fusion approach attempts at developing devices with a high value of Q_p. Compact devices have low values of Q_p of about 0.01. The enhancement of Q_p involves the reduction of end losses in open systems, particularly of high energy ions and electrons.

FUSION ENERGY BALANCE

If E_h is the energy input for heating the plasma, then

$$E_f = Q_p E_h \qquad (2)$$

where Q_p is the plasma power amplification factor.

The E_h variable is also related to the recycle energy for particle injection and heating energy, E_{rec} by

$$E_h = \eta_I E_{rec},$$

or, using Eq. (1),

$$E_{rec} = \frac{E_f}{Q_p \eta_I} \qquad (3)$$

where η_I is the beam injection and plasma heating efficiency.

The term E_h reappears with E_f as output energy from the plasma and is considered to be directed to the thermal conversion cycle.

The fusion energy, E_f, appears as both charged particles energy, E_{cp} and neutron energy, E_n. If f_n is the fraction of fusion energy carried away by the neutrons, then

$$E_n = f_n E_f \tag{4}$$

and

$$E_{cp} = (1 - f_n) E_f \tag{5}$$

As shown in Table 1,

$$f_n(DT) = 0.80,$$
$$f_n(DD) = 0.38.$$

In the fusion blanket, the neutron energy E_n gets multiplied through the breeding and fusion processes by the total Blanket Energy and Multiplication Factor, BEMRF.

The blanket energy output is obtained using Eq. 3 as

$$\begin{aligned} E_b &= BEMRF.E_n \\ &= BEMRF.f_n.E_f \end{aligned} \tag{6}$$

where:

$$BEMRF = BEMR + \frac{Th(n, f) \times 184.2 \frac{MeV}{fission}}{\text{source neutron energy (MeV)}} \tag{7}$$

and

$$\begin{aligned} BEMR &= \text{Blanket Energy Multiplication Ratio} \\ &= \frac{\text{neutron and gamma ray energy deposited in the blanket (MeV)}}{\text{source neutron energy (MeV)}} \end{aligned} \tag{8}$$

Table 2: Comparison of the Energy Deposition Rates and Blanket Multiplication Ratios in a molten salt thorium blanket for different neutron sources [5].

Neutron Source	Neutron Heating Rate (W per n/s)	Gamma Ray Heating Rate (W per n/s)	Total Heating Rate (W per n/s)	Th(n, f) reactions (n/s)	BEMR	BEMRF	Total Energy Deposition (MeV/source neutron)
(Na-Th-F-Be) Molten Salt							
2.45 MeV	1.82×10^{-13}	5.42×10^{-13}	7.24×10^{-13}	7.60×10^{-3}	1.84	2.41	5.90

DT	6.20×10^{-13}	1.12×10^{-13}	1.74×10^{-13}	3.28×10^{-3}	0.77	1.20	16.90
Catalyzed DD	4.01×10^{-13}	8.31×10^{-13}	1.23×10^{-13}	2.02×10^{-3}	0.93	1.38	11.40
(Li-Th-F-Be) Molten Salt							
2.45 MeV	4.42×10^{-13}	4.12×10^{-13}	8.54×10^{-13}	9.80×10^{-3}	2.18	2.92	7.15
DT	9.70×10^{-13}	9.00×10^{-13}	1.87×10^{-13}	3.52×10^{-3}	0.83	1.29	18.14
Catalyzed DD	7.06×10^{-13}	6.56×10^{-13}	1.36×10^{-13}	2.25×10^{-3}	1.03	1.53	12.64

The following values from the calculation results in Table 2 are adopted:

$$BEMRF(DT) = 1.29$$
$$BEMRF(DD) = 1.38$$

Considering the charged particles produced in the fusion process, a factor γ is defined as the fraction of the charged particle energy that folws to the direct energy converter and that is not converted into radiation or conveyed to the thermal conversion cycle.

In the DT system, γ(DT) = 0.0, since direct converters are not normally used. However, for a DD system, γ ranges from a low value of 0.42 for a low-β system to 0.54 for a high-β system. In the calculations that follow, a value of γ(DD) = 0.42 is adopted.

By using Eq. 4, the charged particle energy reaching the direct energy converter is

$$\begin{aligned} E_{cpdc} &= \gamma E_{cp} \\ &= \gamma(1-f_n)E_f \end{aligned} \tag{9}$$

And for the energy reaching the thermal conversion cycle,

$$\begin{aligned} E_{cph} &= (1-\gamma)E_{cp} \\ &= (1-\gamma)(1-f_n)E_f \end{aligned} \tag{10}$$

If η_{dc} is the charged particle conversion efficiency, then the electrical energy output from the direct energy converter is given by

$$\begin{aligned} E_{dc} &= \eta_{dc}E_{cpdc} \\ &= \eta_{dc}\gamma(1-f_n)E_f \end{aligned} \tag{11}$$

If δ is the fraction of energy rejected by the direct energy converter that is recoverable through the thermal cycle, the energy available to the thermal conversion cycle from the direct energy converter is

$$\begin{aligned} E_{dch} &= (1-\eta_{dc})\delta E_{cpdc} \\ &= (1-\eta_{dc})\delta\gamma(1-f_n)E_f \end{aligned} \tag{12}$$

The energy input to the thermal conversion cycle could be converted into electrical energy through an overall thermal cycle efficiency η_{th} as

$$E_{tc} = \eta_{th}(E_{dch} + E_{cph} + E_b + E_h),$$

or, using the equations above,

$$E_{tc} = \eta_{th} E_f \left[(1-\eta_{dc})\delta\gamma(1-f_n) + (1-\gamma)(1-f_n) + BEMRF.f_n + \frac{1}{Q_p} \right] \tag{13}$$

The combined electrical output from the thermal cycle and the direct energy converter will be

$$E_p = E_{tc} + E_{dc} \tag{14}$$

from which an amount E_{rec}, given by Eq. 2, is recycled for particle injection and plasma heating, so that the electrical output capacity for the fusion plant can be written as

$$\begin{aligned} E_{\substack{out \\ (fusion)}} &= E_p - E_{rec} = E_{tc} + E_{dc} - E_{rec} \\ &= E_f \left\{ \eta_{th} \left[(1-\eta_{dc})\delta\gamma(1-f_n) + (1-\gamma)(1-f_n) + BEMRF.f_n + \frac{1}{Q_p} \right] + \eta_{dc}\gamma(1-f_n) - \frac{1}{Q_p \eta_I} \right\} \end{aligned} \tag{15}$$

and the net output is

$$E'_{\substack{out \\ (fusion)}} = E_{\substack{out \\ (fusion)}} .CF_{fusion} \tag{16}$$

where CF_{fusion} is the fusion plant capacity factor.

FISSILE ENERGY AND MATERIAL BALANCES

To determine the electrical energy production from the fission reactors satellites, a material flow balance is performed. The rate of fissile material production in the fusion reactor blanket is

$$\frac{dm_f}{dt} = U.S_n.\frac{M_f}{N_0}C_1 \ (\frac{kg}{year}) \tag{17}$$

where

U = fissile nuclei yield per source neutron

S_n = neutron source strength

M_f = atomic weight of the bred fissile nuclide

N_0 = Avogadro's number

C_1 = conversion factor $=3.15\times10^4(\frac{kg.s}{g.yr})$

The neutron source strength, S_n can be written as

$$S_n = P_f.\frac{1}{E_f}.C_2.CF_{fusion} \tag{18}$$

where

P_f = fusion power

E_f = energy release per fusion event

C_2 = conversion factor = 6.24 $\times$ 10^{18} $(\frac{W.MeV}{MW.J})$

Combining Eqs. 14 and 15 yields

$$\frac{dm_f}{dt} = U.\frac{P_f}{E_f}.\frac{M_f}{N_0}.C_3.CF_{fusion} \tag{19}$$

where

$$C_3 = C_1 \times C_2 .$$

The rate of fissile material consumption, m_c, in the fission satellites converter reactors is given by

$$\frac{dm_c}{dt} = \frac{P_{tc}}{E_{fission}}(1-C)(1+\alpha).\frac{M_f}{N_0}.C_3.CF_{fission} \tag{20}$$

where

P_{tc} = thermal power of the fission converter satellites

$E_{fission}$ = energy release per fission event

C = conversion ratio = $\frac{\text{number of fissile nuclei produced}}{\text{number of fissile nuclei consumed}}$

α = capture to fission ratio= $\frac{\sigma_c}{\sigma_f}$

For steady state operation, the rate of fissile material production should equal the rate of consumption:

$$\frac{dm_f}{dt} = \frac{dm_c}{dt},$$

or

$$\frac{P_{tc}}{E_{fission}}(1-C)(1+\alpha).CF_{fission} = U.\frac{P_f}{E_f}.CF_{fusion}.$$

ENERGY AMPLIFICATION FACTOR AND SUPPORT RATIOS

The energy amplification factor or fission to fusion energy multiplication ℓ, is then given by

$$\ell = \frac{P_{tc}}{P_f} = \frac{E_{fission}}{E_f}.\frac{U}{(1-C)(1+\alpha)}.\frac{CF_{fusion}}{CF_{fission}} \tag{21}$$

Then,

$$P_{tc} = \ell P_f \quad and \quad E_{tc} = \ell E_f \tag{22}$$

where E_{tc} is the energy production over a time interval τ in the fusion and fission reactors.

The electrical output from the fission reactors is given by

$$E'_{\substack{out \\ (fission)}} = \eta_{th,fs}.\ell.E_f.CF_{fission} \tag{23}$$

where $\eta_{th,fs}$ is the thermal cycle efficiency I the fission reactors,

ENERGY AND ELECTRICAL SUPPORT RATIOS

Three figures of merit can be suggested for the assessment of the symbiotic fusion and fission combination.

1. The fission to fusion energy amplification factor ℓ defined by Eq. 18. It measures the multiplication of the energy external to the fusion generators in the fission reactors satellites when the bred fissile fuel releases its energy content.

$$\ell = \frac{E_{fission}}{E_f}.\frac{U}{(1-C)(1+\alpha)}.\frac{CF_{fusion}}{CF_{fission}} \tag{21'}$$

The energy amplification is increased at a first level by the factor

$$\frac{E_{fission}}{E_f} = \frac{190}{17.57} = 10.8, \text{for DT fusion}$$

$$\frac{E_{fission}}{E_f} = \frac{190}{21.62} = 8.8, \text{for Catalyzed DD fusion}$$

The energy multiplication is decreased by the factor containing the capture to fission ratio α given in Table 3 for various nuclides. A choice of the smallest value would favor the energy amplification factor. In this case, the choice of U^{233} in the thorium cycle with a α value of 0.0904 is favored to the choice of U^{235} with a value 0.1701 of or Pu^{239} with a value of 0.3622, in the uranium-plutonium fuel cycle.

Table 3: Nuclear cross section for some fissile and fissionable nuclides at the thermal energy of 0.0253 eV.

Nuclide	Absorption cross section [barn] σ_a	Fission cross section [barn] σ_f	Radiative capture cross section [barn] σ_c	Capture to fission ratio α
Th^{232}	7.4			
Th^{233}	1515	15		
Th^{234}	1.8			
Pa^{233}	41	<0.1		
U^{233}	579.1	531.1	48	0.0904
U^{234}	100.2			
U^{235}	681	582	99	0.1701
U^{236}	5.2			
U^{238}	2.70			
U^{239}	36	14		
Np^{239}	45	<1		
Pu^{239}	1011.5	742.5	269	0.3622
Pu^{240}	289.5	0.030		
Pu^{241}	1377	1009	368	0.3647
Pu^{242}	18.5	<0.2		

1 barn=10^{-24} cm^2.

A much more notable contribution can be noticed by the factor: $\frac{1}{1-C}$, where the conversion factor C is defined as

$$C = \frac{\text{average number of fissile nuclides produced}}{\text{average number of fissile nuclides consumed}}$$

As the value of the conversion factor C approaches unity, an infinite energy multiplication factor ensues:

$$\lim_{C\to 1}\ell = \lim_{C\to 1}\left[\frac{E_{fission}}{E_f}.\frac{U}{(1-C)(1+\alpha)}.\frac{CF_{fusion}}{CF_{fission}}\right]=\infty$$

In more detail, when N nuclei of fissile fuel are consumed, NC nuclei of fertile fuel are converted into fissile nuclei. If the process is repeated, the consumption of N fuel nuclei results in the conversion of a total number of fissile nuclei as:

$$\begin{aligned} N_{total} &= N + NC + NC^2 + NC^3 + NC^4 + ... \\ &= N(1 + C + C^2 + C^3 + C^4 + ...) \\ &= N\frac{1}{1-C}, \forall\ 0 < C < 1. \end{aligned} \tag{24}$$

When C = 1, an infinite amount of fissile fuel can be converted from a starting amount of fertile fuel. When C > 1 the sequence diverges since more than a fissile nucleus is created from a fertile nucleus and cannot be summed mathematically. In this case C is designated as B, the breeding ratio.

If only n recycles are involved, due to the accumulation of undesirable isotopes that could affect the recycling process, Eq. 24 reduces to:

$$\begin{aligned} N_{total} &= N + NC + NC^2 + NC^3 + ... + NC^n \\ &= N(1 + C + C^2 + C^3 + ... + C^n) \\ &= N\frac{1-C^{n+1}}{1-C}, \forall\, 0 < C < 1. \end{aligned} \tag{25}$$

2. The thermal energy support ratio,

$$R = \frac{E_{tc}}{E_{cp} + E_b + E_n}, \tag{26}$$

3. The electrical energy support ratio,

$$S_e = \frac{E'_{out\ (fission)}}{E'_{out\ (fusion)}}, \tag{27}$$

From the derived equations for the energy and material balances, a system analysis can be attempted. The results from a detailed neutronics calculation of a molten salt blanket shown in Table 4 are adopted [5].

Table 4: Fissile and fusile breeding for sodium and lithium salts in DT and DD symbiotic fusion-fission fuel factories. Blanket thickness = 42 cm, reflector thickness = 40 cm; no structure in the salt region.

Source	Li-Be-Th-F Salt						Na-Be-Th-F Salt			
	$Li^6(n,\alpha)T$	**$Li^7(n,n'\alpha)T$**	**$Be^9(n,T)$**	**F(n,T)**	**Total T**	**Th(n,γ)**	**$Be^9(n,T)$**	**F(n,T)**	**Total T**	**Th(n,γ)**
	(Nuclei / fusion source neutron)									
DD 100% 2.45 MeV	0.311	0.001	4.03×10^{-10}	1.01×10^{-7}	0.312	0.579	4.18×10^{-10}	1.04×10^{-7}	1.04×10^{-7}	0.794
DT 100% 14.06 MeV	0.391	0.073	1.08×10^{-4}	3.33×10^{-3}	0.467	0.737	1.04×10^{-4}	3.08×10^{-3}	3.18×10^{-3}	0.966
Catalyzed DD 50% 2.45 MeV 50% 14.06 MeV	0.351	0.037	5.40×10^{-5}	1.67×10^{-3}	0.390	0.658	5.20×10^{-5}	1.54×10^{-3}	1.59×10^{-3}	0.880

A point calculation can be glanced by using the calculated and representative data values listed in Table 5.

Table 5: Parameter values for the symbiotic fusion and fission coupling.

Parameter	Symbol	Catalyzed DD	DT
Beam injection and plasma heating efficiency	η_I	0.80	0.80
Fraction of fusion energy carried by neutrons	f_n	0.38	0.80
Fusion energy output per fusion reaction (MeV/fusion)	E_f	21.62	17.57
Total blanket energy multiplication	BEMRF	1.38	1.29
Fraction of fusion charged particles energy flowing to direct converter	γ	0.42	0.00
Direct conversion efficiency	η_{dc}	0.80	0.00
Fraction of energy rejected by the direct converter recoverable through thermal conversion	δ	1.00	0.00
Fusion thermal conversion cycle efficiency	η_{th}	0.40	0.40
Fission thermal conversion cycle efficiency	$\eta_{th,fs}$	0.30	0.30
Fusion plant capacity factor	CF_{fusion}	0.60	0.60
Fission plant capacity factor	CF_{fision}	0.70	0.70
Energy release per fission event (MeV/fission)	$E_{fission}$	190	190
Capture to fission ratio	α	0.10	0.10
Conversion ratio of converter reactors	C	0.60	0.60
Fissile nuclei yield per source neutron	U	0.880	0.737
Plasma power amplification factor	Q_p	0.01	0.01

THE DIODE ELECTROSTATIC INERTIAL CONFINEMENT, EIC ALTERNATIVE

Earlier work by I. Langmuir and K. B. Blodgett [8] inspired configurations that are electrostatic rather than electrodynamic in nature in the 1960s by Philo T. Farnsworth, the inventor of television and Frequency Modulated (FM) radio, and R. T. Hirsch [8, 9]. They used a diode configuration in the form of spherical screens grids biased to high negative potentials to energize ions and accelerate them to the center of the device, where fusion ensues. This is not attainable with realistic finite size coil conductors.

In its simplest two-grid configuration, the fusion ions such as deuterons are accelerated electrostatically through a nearly spherically symmetric focal point. At the focal point, the beams converge leading to the fusion of the iond confined in the electrostatic potential well.

This configuration was extensively studied by George H. Miley at the University of Illinois. Ion collisions with the grids lead to unavoidable energy losses limiting the power gains to less than 0.1 percent. The University of Illinois Inertial Electrostatic Confinement (IEC) device provides 10^7 2.5 MeV DD neutrons / second when operated with a steady-state deuterium discharge at 70 kV. Being compact and lightweight, the IEC potentially represents an attractive portable neutron source for activation analysis applications, oil well logging, airport luggage and port of entry ship containers inspection for explosive nitrogenous materials and even special fissile materials. The plasma discharge in the IEC is unique, using a spherical grid in a spherical vacuum vessel with the discharge formed between the grid and the vessel wall, while the -70 kV grid (cathode) also serves to extract high-energy ions. A key feature of the IEC discharge is the formation of ion "micro-channels" that carry the main ion flow through the grid openings [10].

IEC is ideally suited for burning advanced neutronless fuels such as D-He^3 and p-B^{11} due to the beam-like energy and low electron temperature. Energetic fusion products escape the well and can undergo direct conversion to electricity.

The Star Mode Inertial IEC is a simple and lightweight device. The charged particles beams are focused through large openings to minimize the interception of grid wires and give a good focus despite deviations from the spheroid shapes.

The preliminary design of a small 100-kWe p-B^{11} space power unit was undertaken along with the possible extension to an ion thruster for space applications. Difficulties to be addressed include being able to scale up to higher powers needed for more ambitious future space missions. The objective would be to use a fusion powered IEC for next generation power units in the 100-kWe range. The technology underlying the electrically-driven IEC jet unit underpins the development of a next generation fusion ion propulsion units for deep space spacecraft replacing chemical systems.

A Modular approach takes advantage of inherently small size of the IEC units. In a Magnetically Channeled Spherical Array (MCSA) the linked units have improved confinement and guide fusion products out of the system. A null-field region created within each pair of Helmholtz coils confine plasma which is confined by the peripheral magnetic field and no grid structure. A cusp field configuration provides fluid stability. The radial leakage is recirculated back into the confinement region and the axial leakage is retrapped in the neighboring cells.

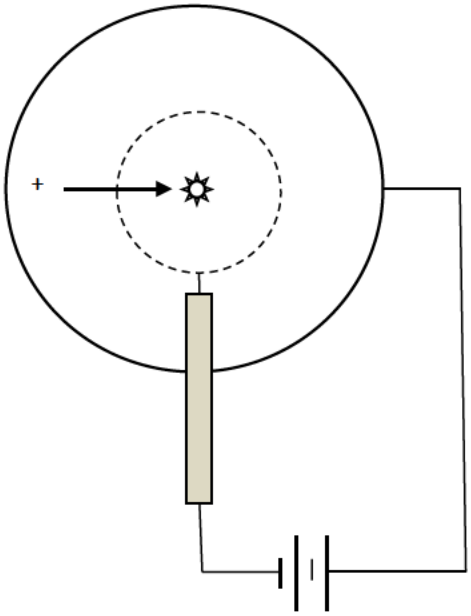

Figure 3. Simple two-grid diode IEC device configuration as a single diode.

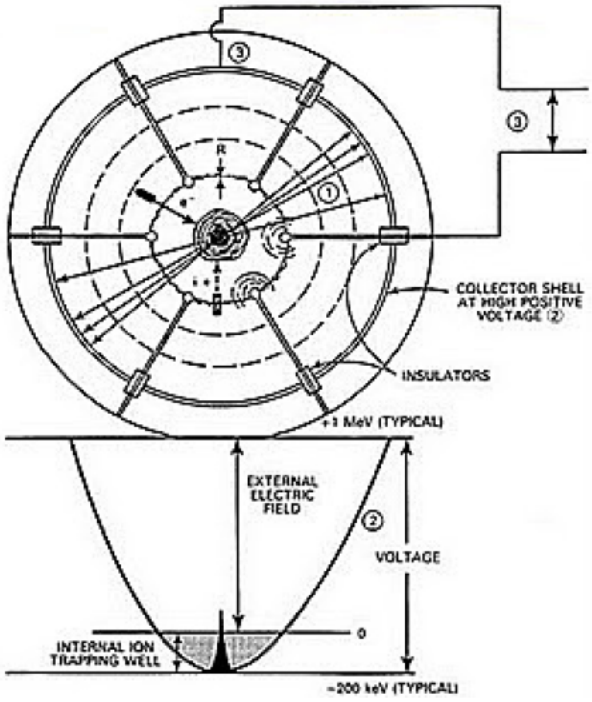

Figure 4. Direct energy conversion can be achieved with grid collection of the charged particles[12].

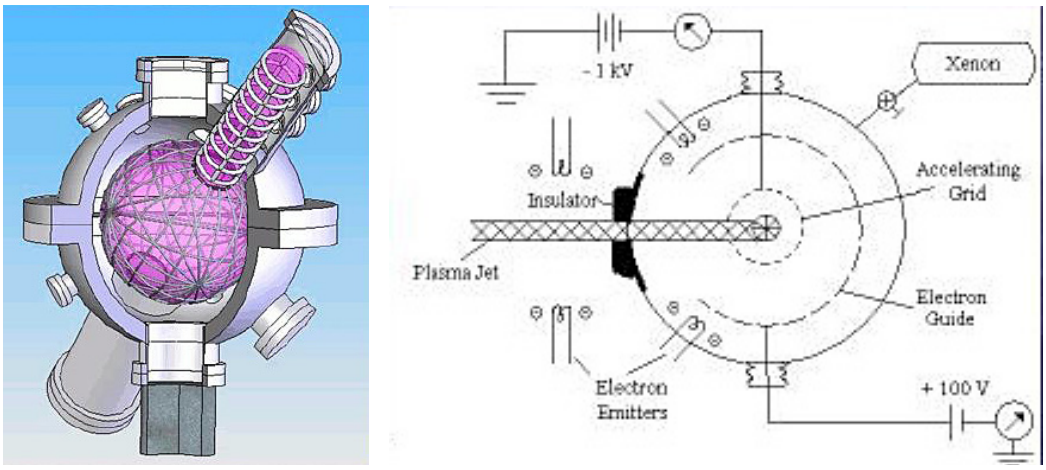

Figure 5. Inertial Electrostatic Confinement IEC device operating in the jet mode. The Specific Impulse I_{sp} = 3,000 sec, Input power = 750-800 Watt, Thrust T = 34 mN, Accelerating potential = 600 V, Jet power: P_{jet} = 500 Watts, Efficiency: h_t = 62-68 percent [10].

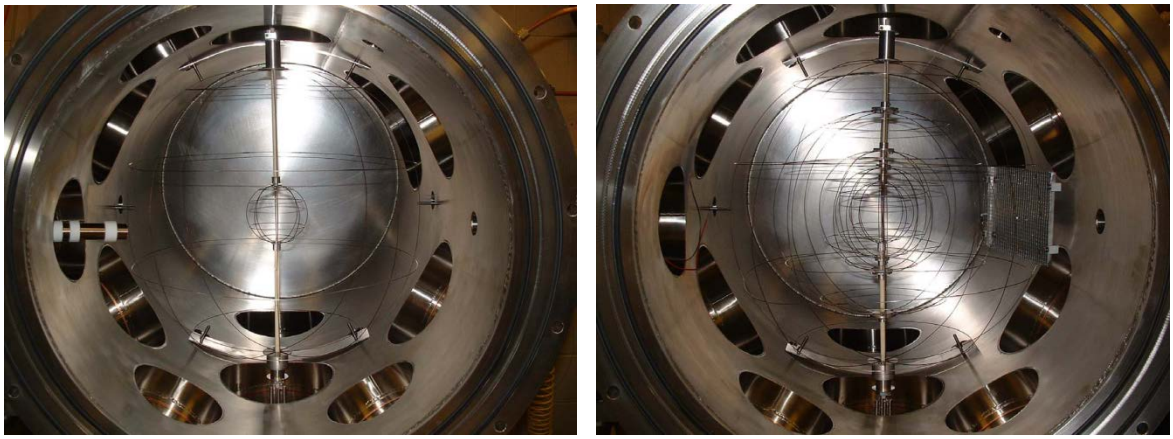

Figure 6. Two-grid and Multigrid systems shown in their vacuum chambers [13].

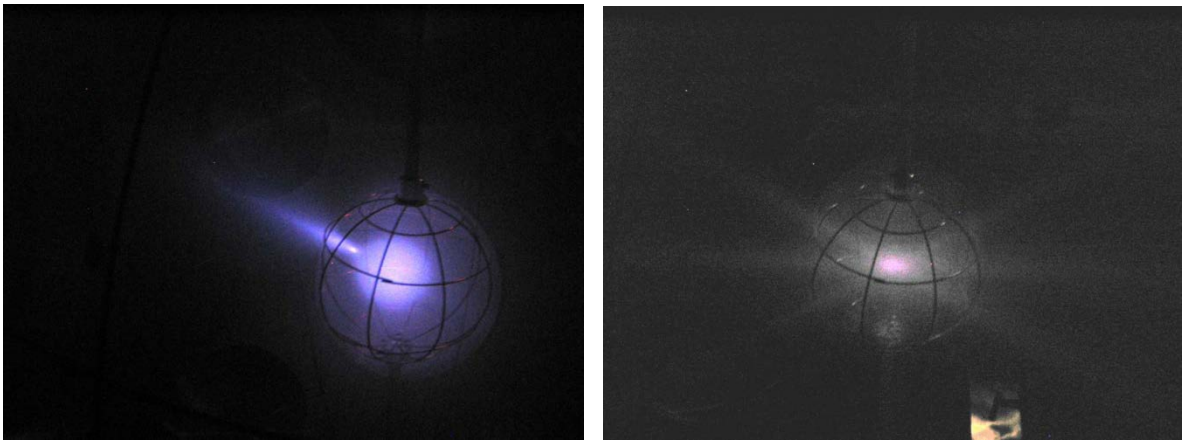

Figure 7. Two grid system jet and star plasma modes [13].

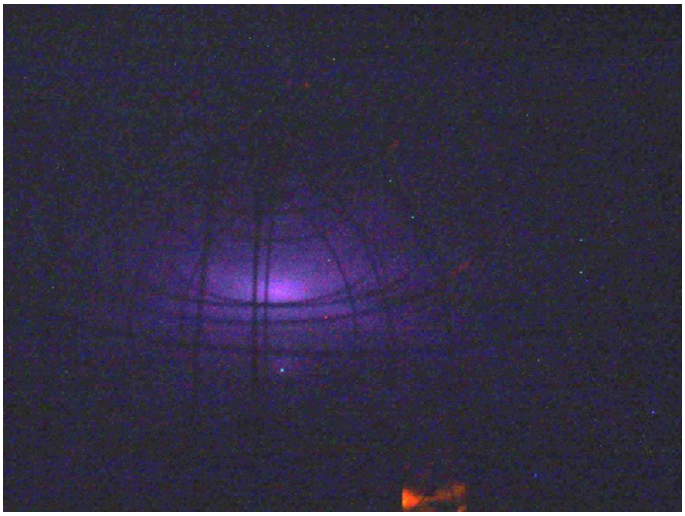

Figure 8. Multigrid system star mode of operation [13].

A presumption is that the grid configuration cannot generate net power because the confined ions collide with the grid too often before they get to the center where they would fuse. Magnetically shielding the grid may allow the ions to accelerate to the center with less grid collision rates. On the other hand, in the grid design, the fast ions also lose their energy and thermalize through multiple scattering collisions with the cold background medium. Other mechanisms would be ions sputtering from the outer shell and accelerating back to the grid, and electron accelerating away from the grid to the shell. A design factor to be considered is the need for cooling the central cathode to prevent it from melting in a power production application.

ELECTRODYNAMIC INERTIAL CONFINEMENT, EIC

Using a cusped configuration, energetic electrons are trapped in a quasi-spherical polyhedral magnetic field to create a spherical electric potential well in which ions can be dropped. If injected at its edge, they are accelerated to the center with an increase in density and kinetic energy and inducing fusion. In this approach, the power loss problem is shifted from being an ion grid collision problem into electron transport losses across high magnetic fields to the confining magnets. The competing electron power loss and the fusion energy gain are decoupled and can be optimized

Cusp-axis fields of 70-100 Gauss were generated and DD fusion did occur. Deep electron created wells at 27 kV well depth, and were created with -30 kV electron drives [4].

CUSPED MAGNETIC FIELD CONFIGURATIONS

In most systems in which a plasma is confined by a magnetic field that surrounds it smoothly without a discontinuity, there is a tendency toward the creation of instabilities. This is so because the magnetic lines of force which are stretched around the plasma can shorten themselves by burrowing into the gas and thus force it outward.

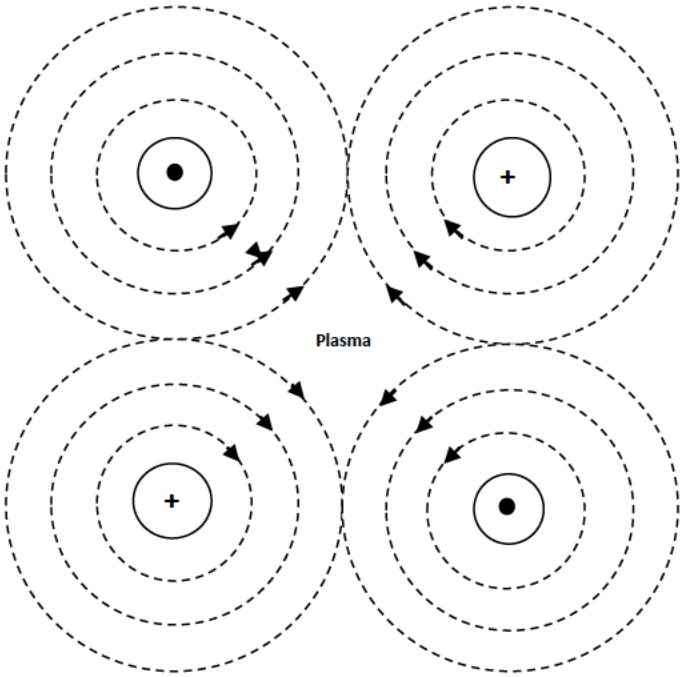

Figure 9. Linear cusp magnetic field configuration produced by an array of four straight line currents in wires alternating in direction.

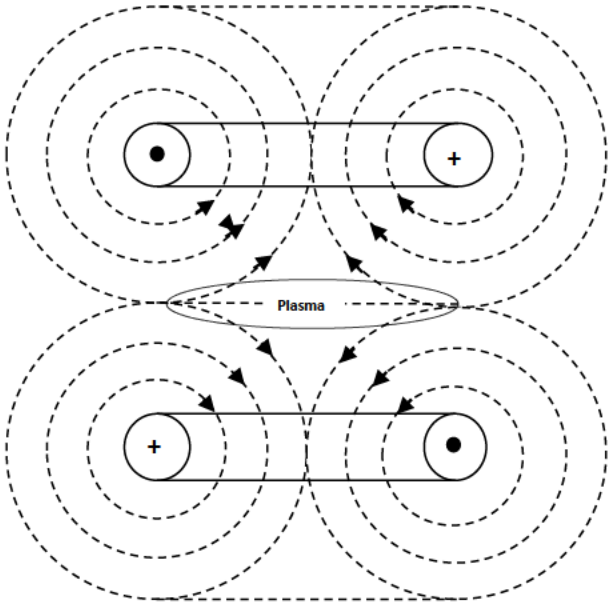

Figure 10. Biconal cusp magnetic field configuration produced by two parallel toroidal coils or magnets with currents flowing in opposite directions.

A confinement system which is absolutely stable against arbitrary deformations, even of finite amplitude, of the plasma can be obtained if the magnetic field lines curve away everywhere from a diamagnetic plasma. This means that the magnetic field and plasma interface is

everywhere convex on the side toward the plasma. To satisfy this curvature requirement, the magnetic field must possess cusps, which are points or lines, or both, through which the magnetic field lines pass radially outward from the center of the confinement region as shown in Figs. 9, 10.

A laboratory geometry of this kind is called a picket fence, and consists of two layers of parallel wires carrying currents in alternating directions so that the magnetic field has a series cusps. The magnetic fields are generated in the vicinity of the walls decreasing the power needed in maintaining them. This advantage is superseded by the more important advantage of stable confinement.

Another type of cusped geometry is the biconal cusp produced by a pair of magnetic field circular coils with the currents in them flowing in opposite directions. A succession of cusped configurations can generate a toroidal cusped system.

If there is a loss of plasma from the central volume, the lines of force would have to stretch to fill the volume previously occupied by the plasma. Since this requires extra energy expenditure, this type of instability would not probably occur.

In the cusped configuration, a singular condition exists at the center where the magnetic field goes exactly to zero. A particle passing through this point will experience a large field change occurring in a time interval less than the gyromagnetic period, particularly as this period is lengthened by the decrease in the magnetic field strength. The magnetic moment becomes no longer an adiabatic invariant of the system.

In the special case of a particle actually passing through the point where the magnetic field is zero, the particle will momentarily travel in a straight line and its motion will bear no relationship to that before its passage through this point. The magnetic energy of the particle can theoretically reach an *infinite* value along the zero magnetic field line.

If one considers a confined plasma rather than a particle, one must consider the problem of Magneto Hydro Dynamic (MHD) cumulation of energy near a zero field line.

Let us consider a perfectly conducting and incompressible cylindrical plasma to be immersed in a quadrupolar steady external magnetic field:

$$\bar{B}_e = B_0 \nabla \bar{x}\, \bar{y}\,. \tag{28}$$

In the absence of currents and velocities the plasma is under an unstable equilibrium to a linear velocity perturbation:

$$\begin{aligned} v_x &= U\bar{x}, \\ v_y &= U\bar{y}. \end{aligned} \tag{29}$$

The MHD equations of motion which do not depend on the z axis variable can be exactly solved with the velocity perturbation as an initial condition.

The motion generates an axial current j_z in the z direction. Due to the pinch effect or the Lorentz force:

$$\bar{F} = \bar{j} \times \bar{B}\,, \tag{30}$$

the circular section of the cylinder is deformed into ellipses of axes (0x, 0y). After a time comparable to the ratio of the initial cylinder ration to the Alfvèn velocity:

$$V_A = \frac{B_0}{\left(4\pi\rho\right)^{1/2}} \tag{31}$$

a cumulation process occurs and the elliptical cross section is stretched along the x axis or the y axis depending on the relative values of the initial perturbation velocities U and V.

The important result is that the plasma flattens and expands radially perpendicular to the z axis while the plasma kinetic energy and the current density increase without limit.

The MHD equations can also be solved if the plasma is considered to be a perfect gas with a finite electrical conductivity. At the finite cumulation time, the plasma initially contained within a circular cross section plasma would be squeezed within an ellipse of zero volume. The density, velocity V_y, current density j_z, as well as the internal kinetic or magnetic energies, all become infinite inside the limiting segments.

The cumulation process requires an energy source supplied by the energy stored in the magnetic field. An interesting consequence of the cumulation process is that the electron velocity J/n tends to infinity which could explain the process of acceleration of particles to extremely high velocities as is observed in cosmic ray particles. This suggests their origin as magnetic field configurations occurring in Gamma Ray Bursts (GRBs).

The hot plasma in the magnetic field would generate high energy radiation in the form of synchrotron radiation.

PLASMA STABILITY AND THE BETA FACTOR

The pressure in a plasma of density as a function of its temperature T in Kelvins and the Boltzmann constant k is

$$p_{plasma} = nkT \tag{32}$$

The pressure exercised on the plasma by the containing magnetic field B is

$$p_{magnetic} = \frac{B^2}{2\mu} \tag{33}$$

The beta value is defined as the ratio of the plasma pressure to magnetic pressure

$$\beta = \frac{p_{plasma}}{p_{magnetic}} = \frac{nkT}{(B^2/2\mu)} \tag{34}$$

The beta parameter is a measure of the kinetic to electromagnetic energy content of a plasma. There is a limit on the value of beta before instabilities that would lead to the destruction of the plasma would occur.

WIFFLE BALL CONFIGURATION

Born in 1928, Robert W. Bussard was an American physicist working primarily in nuclear fusion energy research. He received his Ph. D. from Princeton University. He was as co-founder and director of Energy/Matter Conversion, EMC2 Corporation. He held the post of Assistant Director to the USA Atomic Energy Commission and positions at Los Alamos National Laboratory (LANL), Oak Ridge National laboratory (ORNL), and the TRW Systems Company, a defense contractor. He acted as a designer of the Nerva motor, a government-sponsored project to develop a nuclear powered rocket for heavy-lift applications in the late 1960's.

Bussard is known for conceiving the Bussard ramjet, an interstellar spacecraft powered by hydrogen fusion using hydrogen collected from the interstellar gas medium utilizing a magnetic field.

He spent over 20 years developing a modified Farnsworth-style “Polywell” compact fusion device, successfully generating over 100,000 times the output of Farnsworth's original experiments. In 2006, Bussard's Polywell design was awarded the Outstanding Technology of the Year Award by the International Academy of Sciences.

The “Bussard Ramjet” is a modified fusion-drive starship proposed in the 1960's by Carl Sagan and further popularized by authors such as Jerry Pournelle and Larry Niven.

Bussard became disenchanted with the magnetic toroidal confinement Tokamak and Stellarator fusion concepts. He returned to the roots of Farnsworth-style fusion in the “Polywell” project that he initiated in 1986. He was funded for over 20 years by the Department of the Navy. Bussard's EMC2 Corporation was tasked with solving 19 fundamental challenges that stood in the way of designing commercially viable Farnsworth “fusors.” Bussard's first intended application was an 8-foot diameter naval reactor capable of generating 100 MWth of output power.

Bussard's Polywell design is conceived for portability, making it perfect for not only the Navy's intended use in powering ocean vessels and submarines, but also for providing high output thrust for proposed nuclear space-applications for high velocity trans-orbital spacecraft capable of reaching the moon in 8 hours.

The 100 MWth nominal power is to insure getting above break-even conditions. It can be run at lower power. Thermal problems get worse with larger sizes. The fusion reactor is a geometrical problem, more so than a fission reactor. Size does matter, and building a large unit insures that there is margin for error.

The device uses a cusped fusion configuration. The earliest device was constructed in 1994 and named Wiffle Ball 2 or in short WB2. Another Polywell device designated as WB4 was constructed in 2003. These devices suffered from excessive electron losses. The WB6 device controlled the electron losses in 2005.

After Bussard's death, the USA Navy went on to fund the construction of a device designated as WB7. It was constructed, saw its first plasma generation in January of 2008, and met expectations. The USA Navy was interested in the construction of a 100 MWth power reactor for naval propulsion applications.

Figure 11. Wiffle Ball toy.

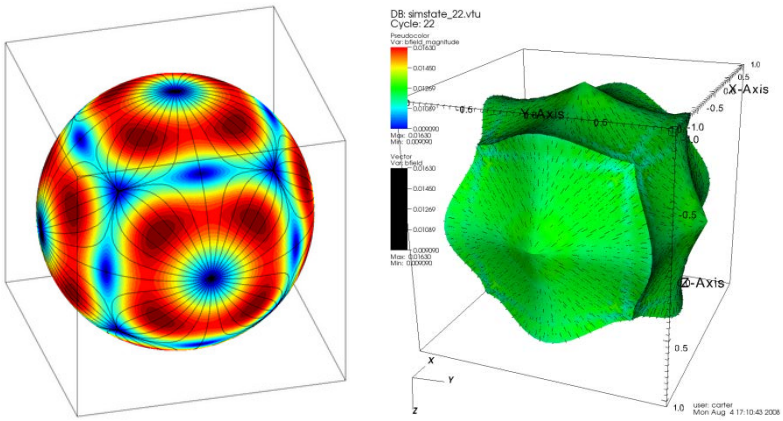

Figure 12. The Wiffleball cusped magnetic fields configuration [14].

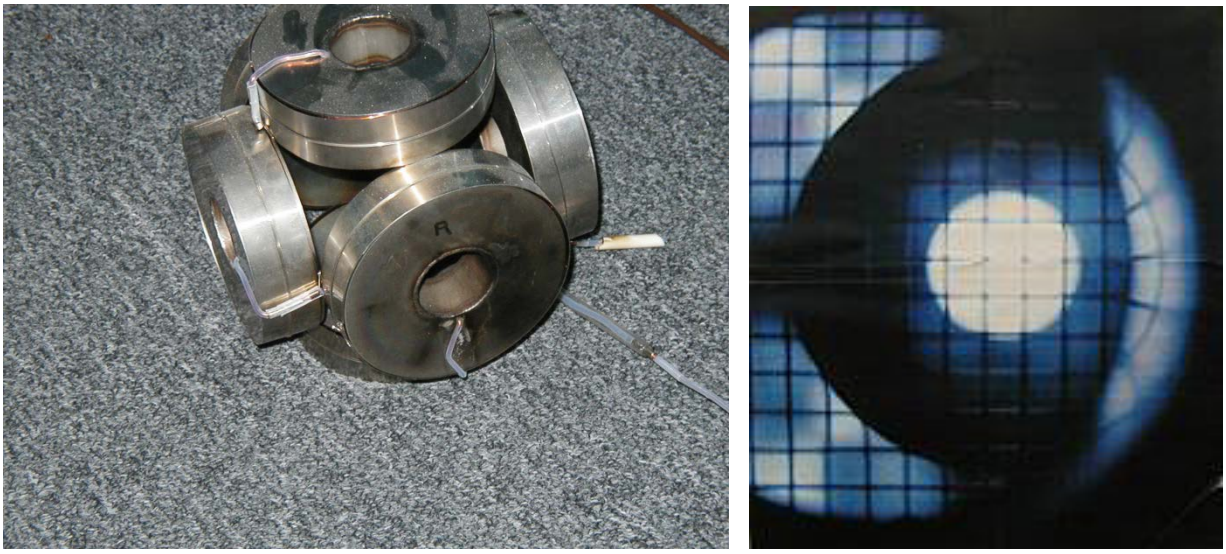

Figure 13. Cusped configuration Wiffle Ball WB2, 1994. Source: EMC2 Corporation [4].

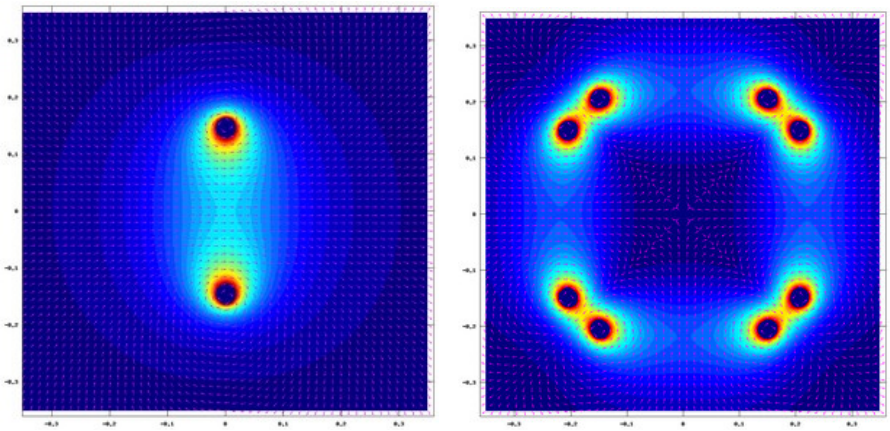

Figure 14: Magnetic fields from single and six current loops.

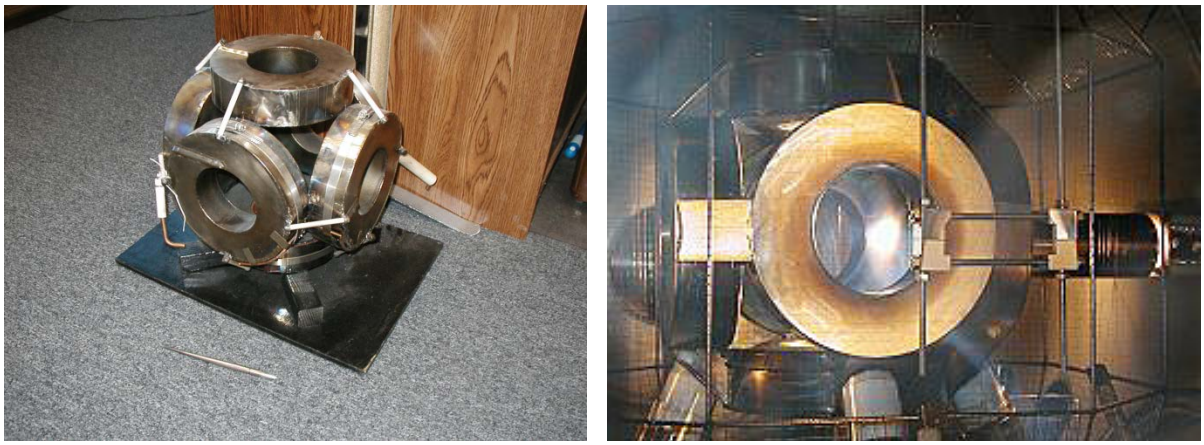

Figure 15. Polywell fusion Wiffle Ball WB4 device, 2003. Source: EMC2 Corporation [4].

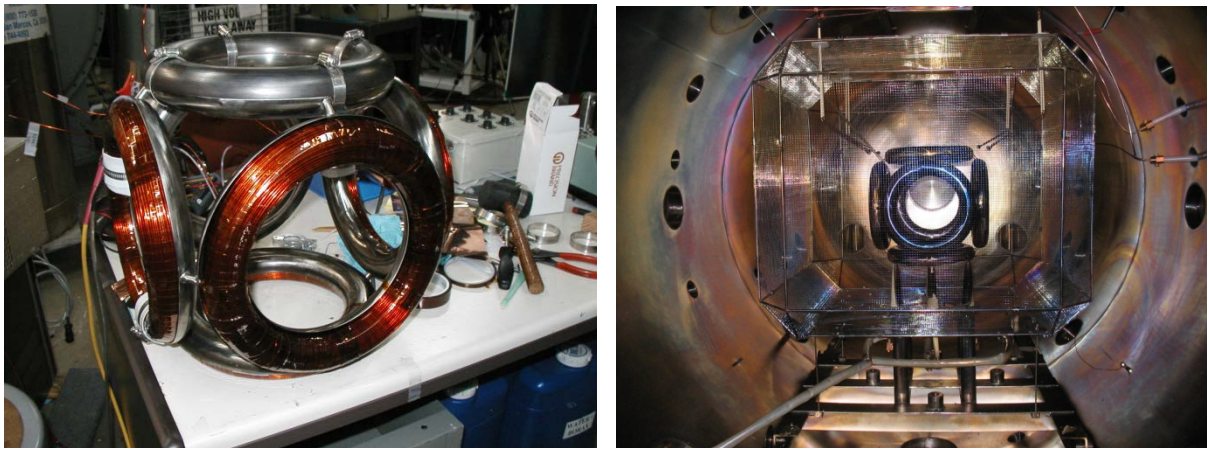

Figure 16. Wiffle Ball WB6 device achieved control of electron losses, 2005. Source: EMC2 Corporation [4].

Figure 17. Wiffle Ball WB7 device using a He plasma. Source: EMC2 Corporation [4].

WIFFLEBALL EXPERIMENTAL DEVICES

Bussard and his team at Energy/Matter Conversion Corporation, over 20 years of research, explored the possibility of a neutronless pure fusion process.

The fusion process favored by Bussard uses the pB^{11} fusion reaction producing a C^{12} nucleus in its excited state. This excited C^{12} nucleus decays to Be^8 and He^4. Be^8 within 10^{-13} sec further decays into two more He^4 nuclei. This is the only known nuclear-energy releasing process that releases fusion energy and three helium atoms, but no initial neutrons.

$$
\begin{aligned}
&{}_1H^1 + {}_5B^{11} \rightarrow {}_6C^{12*} \\
&{}_6C^{12*} \rightarrow {}_4Be^8 + {}_2He^4(3.76\,MeV) \\
&{}_4Be^8 \rightarrow {}_2He^4(2.46)\,MeV) + {}_2He^4(2.46MeV) \qquad (35) \\
&\text{---------------------------------------} \\
&{}_1H^1 + {}_5B^{11} \rightarrow 3_2He^4 + 8.682\ MeV
\end{aligned}
$$

This reaction appears to be radiation-free, but even though it is 2-4 orders of magnitude less in terms of neutron production than the DT reaction, some side radiation producing reactions do occur, such as:

$$
\begin{aligned}
&{}_1H^1 + {}_5B^{11} \rightarrow {}_6C^{11} + {}_0n^1 - 2.8\,MeV \\
&{}_1H^1 + {}_5B^{11} \rightarrow {}_6C^{12} + \gamma + 16\,MeV \\
&{}_1D^2 + {}_5B^{11} \rightarrow {}_6C^{12} + {}_0n^1 + 13.7\,MeV \\
&{}_2He^4 + {}_5B^{11} \rightarrow {}_7N^{14} + {}_0n^1 + 0.157\,MeV \\
&{}_2He^4 + {}_5B^{11} \rightarrow {}_6C^{14} + {}_1H^1 \\
&{}_2He^4 + {}_5B^{11} \rightarrow {}_6C^{12} + {}_1T^3
\end{aligned}
$$

Some reactions will also occur with any B^{11} impurity, and a few energetic product alpha particles will interact with the wall materials, producing neutrons.

For the overall reaction, the atomic masses of the isotopes are:

$$m({}_1H^1) = 1.0078250\,amu$$
$$m({}_5B^{11}) = 11.0093055\,amu$$
$$m({}_2He^4) = 4.0026032\,amu$$

The Q-values of the overall reactions is:

$$Q = (1.0078250 + 11.0093055 - 3\times 4.0026032)amu \times 931.481\frac{MeV}{amu} = 8.682\,MeV$$

The pB^{11} reaction is reported to have a resonance with a cross section of 0.1 b (barn) at 50 kV drive and an absolute peak of 1.2 b at 200 kV nominal drive voltage that could be used to enhance its occurrence. Six low energy electrons are released from the ionized hydrogen and boron fuel atoms which loose them around 0.67 keV. They thermalize quickly and replace other electron losses. The size of an eventual reactor using this reaction is estimated at 3 m^3 compared with 1 m^3 for a reactor using DT fuel.

The reactor power output increases with a stronger magnetic field and a smaller radius, and is reported to scales as:

$$P\ \alpha_\ell\ \frac{B^4}{r^3}$$

or:

$$\frac{P}{P_0} = \left(\frac{r_0}{r}\right)^3 \left(\frac{B}{B_0}\right)^4$$

where B is the magnetic field strength

r is the plasma radius

The power gain is reported to scale as:

$$G\alpha_\ell \frac{B^4}{r}$$

As a reference value, we can take a power output of P_0 = 10 MWth with r_0 = 0.15 m plasma and a B_0 = 0.5 Tesla (T) magnetic field.

With 10 times the size of the 0.15 m plasma at 1.5 m, and ten times the 0.5 T magnetic field at 5 T, the power would be 10 times the reference value as:

$$P = 10\left(\frac{0.15}{1.5}\right)^3\left(\frac{5}{0.5}\right)^4 = 10\times10^{-3}\times10^{+4} = 100\,MWth$$

The most commonly studied fusion process today is the reaction that occurs between deuterium and tritium DT reaction that produces helium and a fast neutron. Various magnetic confinement configurations have been designed and developed over the years to contain the high-energy DT fusion reaction. The Tokamak is one such magnetic confinement vessel, 30 m across by 110 feet tall. The Stellarator, the Tandem Mirror, and the Spheromak are other configurations [1].

Electrostatic or electrodynamic confinement can easily achieve high temperature plasmas, but low density. On the other hand, magnetic confinement devices can achieve high densities, but high temperatures are difficult to obtain. Electrostatic and electrodynamic devices are compact in size, and hence cost less compared to the larger sizes of Tokamak and Stellarator devices.

In the fusion process, the reacting nuclei must overcome the Coulomb barrier repulsion between them. Since the Coulomb energy barrier increases in height with increasing atomic number, fusion reactions with low Z number nuclei can occur easier than with heavier nuclei.

The three possible reactions with hydrogen H nuclei:

$$\begin{aligned} {}_1H^1 + {}_1H^1 &\rightarrow {}_1D^2 + {}_{+1}e^0 + \nu_e \\ {}_1H^1 + {}_1D^2 &\rightarrow {}_2He^3 + \gamma \\ {}_1H^1 + {}_1T^3 &\rightarrow {}_2He^4 + \gamma \end{aligned} \qquad (36)$$

where ν_e is an electron neutrino, are known to have reaction cross sections too small to permit a net gain of energy at the technologically attainable temperatures.

Thus one has to go to the next most abundant isotope, deuterium with its DD reaction possessing a neutron and a proton branches:

$$\begin{aligned} {}_1D^2 + {}_1D^2 &\rightarrow {}_1T^3(1.01\ MeV) + {}_1H^1(3.02 MeV) + 4.03\ MeV \\ {}_1D^2 + {}_1D^2 &\rightarrow {}_2He^3(0.82\ MeV) + {}_0n^1(2.45 MeV) + 3.27\ MeV \end{aligned} \qquad (37)$$

For first generation fusion reactors, the DT reaction is considered as the easiest to achieve, since it requires the lower plasma temperature to be achieved:

$${}_1D^2 + {}_1T^3 \rightarrow {}_2He^4(3.52\ \text{MeV}) + {}_0n^1(14.1\ \text{MeV}) + 17.59\ \text{MeV} \qquad (38)$$

The 17.59 MeV energy release from this reaction is equivalent to 94,000 [kW.hr/gm] of DT fuel.

The He^3 produced in the neutron branch of the DD reaction can react with deuterium in a reaction producing charged particles and no neutrons as:

$${}_1D^2 + {}_2He^3 \rightarrow {}_2He^4(3.6\ MeV) + {}_1H^1(14.7\ MeV) + 18.3\ MeV \qquad (39)$$

In a fusion reactor using deuterium, the four last reactions should be expected to occur simultaneously in what is designated as the Catalyzed DD reaction, where six deuterons are fused with a release of energy of 43.2 MeV, or 43.2/6 = 7.2 MeV per deuteron: Tritium and He^3 act as catalysts in the overall reaction.

$$
\begin{aligned}
&{}_1D^2 + {}_1D^2 \rightarrow {}_1T^3 + {}_1H^1 + 4.03\ MeV \\
&{}_1D^2 + {}_1D^2 \rightarrow {}_2He^3 + {}_0n^1 + 3.27\ MeV \\
&{}_1D^2 + {}_1T^3 \rightarrow {}_2He^4 + {}_0n^1 + 17.6\ MeV \\
&{}_1D^2 + {}_2He^3 \rightarrow {}_2He^4 + {}_1H^1 + 18.3\ MeV \\
&\text{---------------------} \\
&6\,{}_1D^2 \rightarrow 2\,{}_1H^1 + 2\,{}_2He^4 + 2\,{}_0n^1 + 43.2MeV
\end{aligned}
\qquad (40)
$$

For kinetic reactions temperatures below 50 keV the DHe^3 reaction is not significant and the energy release would be 43.2 - 18.3 = 24.9 with each of the five deuterons contributing an energy release of 24.9/5 = 4.98 MeV.

$$
\begin{aligned}
&{}_1D^2 + {}_1D^2 \rightarrow {}_1T^3 + {}_1H^1 + 4.03\ MeV \\
&{}_1D^2 + {}_1D^2 \rightarrow {}_2He^3 + {}_0n^1 + 3.27\ MeV \\
&{}_1D^2 + {}_1T^3 \rightarrow {}_2He^4 + {}_0n^1 + 17.6\ MeV \\
&\text{---------------------} \\
&5\,{}_1D^2 \rightarrow {}_1H^1 + {}_2He^3 + {}_2He^4 + 2\,{}_0n^1 + 24.9MeV
\end{aligned}
\qquad (41)
$$

Whereas deuterium (D) occurs in the water in the oceans and can be extracted through electrolysis or distillation, tritium (T) does not appreciably occur in nature since it is radioactive with a half life of 12.34 years. Tritium has to be produced or bred from the isotopes of lithium through interaction of the neutrons produced in the fusion reactions with lithium surrounding the fusion reaction in the form of a blanket. Lithium or its compounds could also be used as a coolant absorbing the 14.1 MeV of energy carried out by the fusion neutrons.

Natural lithium occurs as 7.5 percent of the ${}_3Li^6$ and 92.5 percent as the ${}_3Li^7$ isotope. An exothermic reaction can occur by thermal neutrons with the first isotope and an endothermic reaction by fast neutrons with the second isotope as follows:

$$
\begin{aligned}
&{}_3Li^6 + {}_0n^1(\text{thermal}) \rightarrow {}_2He^4(2.05\ \text{MeV}) + {}_1T^3(2.73\ \text{MeV}) + 4.78\ \text{MeV} \\
&{}_3Li^7 + {}_0n^1(\text{fast}) \rightarrow {}_2He^4 + {}_0n^1 + {}_1T^3 - 2.47\ \text{MeV}
\end{aligned}
\qquad (42)
$$

The DT reaction produces neutrons that can activate the structure of the reactor, creating some radioactivity.

A fast neutron from the fusion reaction can in principle produce two tritons in these two reactions, sine it is re-emitted from the fast reaction, and is available, if not absorbed by other nuclei, to induce the second reaction at low energy.

Some other potential fusion reactions with their branching ratios estimated at their cross section peaks are shown in Table 6.

Table 6: Fusion Reactions and their energy releases [13].

Reactants	Branching Ratios [percent]	Products	Energy yield [MeV]	Energy yield [Joule]
$_1D^2 + _1D^2$ (proton branch)	50	$_1T^3$ (1.01 MeV) + $_1p^1$ (3.02 MeV)	4.03	6.460×10^{-13}
$_1D^2 + _1D^2$ (neutron branch)	50	$_2He^3$ (0.82 MeV) + $_0n^1$ (2.45 MeV)	3.27	5.240×10^{-13}
$_1D^2 + _1T^3$		$_2He^4$ (3.54 MeV) + $_0n^1$ (14.06 MeV)	17.60	2.818×10^{-12}
$_1D^2 + _2He^3$		$_2He^4$ (3.66 MeV) + $_1p^1$ (14.6 MeV)	18.3	2.930×10^{-12}
$_1T^3 + _1T^3$		$_2He^4 + 2\ _0n^1$ + 11.3MeV	11.3	1.810×10^{-12}
$_2He^3 + _1T^3$	51	$_2He^4 + p + _0n^1$ + 12.1MeV	12.1	1.940×10^{-12}
	43	$_2He^4$ (4.8 MeV) + $_1D^2$ (9.5 MeV)	14.3	2.292×10^{-12}
	6	$_2He^4$ (0.5 MeV) + $_0n^1$ (1.9 MeV) + $_1p^1$ (11.9 MeV)	14.3	2.292×10^{-12}
$_1p^1 + _3Li^6$		$_2He^4$ (1.7 MeV) + $_2He^3$(2.3 MeV)	4.02	6.440×10^{-13}
$_1p^1 + _3Li^7$	20	$2\ _2He^4$ + 17.3MeV	17.3	2.773×10^{-12}
	80	$_4Be^7 + _0n^1$ - 1.6 MeV	-1.6	-2.565×10^{-13}
$_1D^2 + _3Li^6$		$2\ _2He^4$ + 22.4 MeV	22.4	3.391×10^{-12}
$_1p^1 + B^{11}$		$3\ _2He^4$ + 8.68 MeV	8.68	1.390×10^{-12}
$_2He^3 + _3Li^6$		$2\ _2He^4$ + p + 16.9 MeV	16.9	
$_0n^1$ (thermal)+ $_3Li^6$		$_2He^4$ (2.05 MeV) + $_1T^3$ (2.73 MeV)	4.78	7.660×10^{-13}
$_0n^1$ (fast)+ $_3Li^7$ (endothermic		$_2He^4$ (2.1 MeV) + $_1T^3$ (2.7 MeV)	- 2.47	-3.96×10^{-13}
$_2He^3 + _2He^3$		$_2He^4 + _1p^1 + _1p^1$	12.9	2.065×10^{-12}

The majority of the fusion processes under investigation are expensive, costing billions of USA dollars; require giant machines; and offer no predictability. Nonetheless, we know that fusion works because every star is a fusion reactor. The fusion reactors of the stars and the sun are held together by a direct force field. This works very well and efficiently. This force field is gravity. Gravitational forces between particles draw them directly together. Only one other force is known to be like gravity: this is the electric field force or "coulomb" force, between electrically-charged particles.

Charged particles of opposite signs attract each other with direct forces; charged particles in electric fields feel forces directly along field gradients. Thus, fusion fuel plasmas could be held together efficiently by electric forces and electric fields. This is called “Electrostatic Inertial Confinement Fusion” or “Electrodynamic Inertial Confinement Fusion.”

Bussard was not the first to try to create such a field. One notable technique acted as a diode and utilized a spherical screen grid that was biased to a positive potential, thereby attracting electrons through the screen, producing a negative potential well. As the electrons passed through the screen, they slowed down as their kinetic energy was transformed into potential energy in the potential well, and ions could then be dropped into it at the edge, fall down, and be recirculated back and forth. Any particles not reacting went back into the well. The only problem with this method was that the grid was not transparent. Because of the high interception rate on the grid, essentially all of the energy put into the electron acceleration went into the grid. Energy was lost and the grid melted.

Bussard's invention, however, removes the diode grid and replaces it with a magnetic field. It is known that magnetic fields do not contain neutral plasmas very well, as in the case of the Tokamak. Magnetic fields, however, contain electrons very easily because electrons are extremely light.

The basic approach of electrodynamic inertial fusion follows these steps:

1. A quasi-spherical cusped magnetic field trap is generated using circular coils or magnets. These could permanent, electrical or superconductiong magnets.
2. Energetic electrons are injected into the cusp to form a spherical negative potential well.
3. The fusion ions trapped in this spherical well are focused through the central region and oscillate across the "core" until they are fused.
4. The device acts like a spherical colliding beam device.
5. Fuel gas is fed at the potential well edge. The fusion products escape to the system walls.
Ion fusion power generation occurs in the central region. The deposited ions at the periphery can lead to direct energy conversion into electricity.
6. The electron drive power is decoupled from the fusion process.
7. The power balance is affected by injected electron losses; the main losses occurring through the magnetic cusps and to the device's walls. Thus the magnetic confinement of the electrons is critical to the success of the device.

The "Wiffle Ball" (WB) concept insures cusp sealing and the magnetic insulation of the walls is important. The Wiffle Ball is a toy consisting of perforated spherical shell with a ball bearing bouncing within it. The electrons will bounce back and forth within the magnetic ball until they find a hole at some bounce from which they can escape.

The recirculating machine with magnetically protected coil surfaces is designated as a Magnetic Grid or "Magrid" (MG) effect machine and reduces power losses and increases the energy gain. The cusp axis flow does not need to be a loss if the device is open and the electrons can recirculate along the cusp axes to the outside of the machine. The machine itself is thus required to be placed at the center of a containing wall or shell that is kept at a potential below that of the machine proper, by the voltage used to drive the electron injectors.

In 1994, Bussard successfully demonstrated a Wiffle Ball (WB) configuration, achieving a beta-1 condition. In 2005, he was able to magnetically insulate the electrons from the walls via his "Magrid" transporter.

Early prototype experienced some losses because the original coils touched one another, resulting in intersecting magnetic fields. This made the magnetic field lines run into the metal vessel walls resulting in electron losses. Bussard realized that all the coil containers had to be conformal to the magnetic fields they produced. If he utilized circular toroidal coils spaced at the corners, the magnetic fields could be allowed to go out between the coils. Using such a device, that offered both the Wiffle Ball effect and the Magrid transporter, Bussard was able to achieve $1x10^9$ fusions/second for 0.25 milliseconds.

The Wiffle Ball fusion reactor design uses six metal rings joined to form a cube with one ring on each side. For a 100 MWth reactor, each ring would be about a yard in diameter. Each ring would have copper wires wound into an electromagnet. Permanent magnets using rare earths alloys such as neodymium may be possibly used if enough strength can be achieved. The whole device is emplaced inside a vacuum chamber.

Upon being energized, the magnets generate a cusped magnetic field into which electrons from an electron gun are injected. The magnetic field squeezes the electrons into a dense ball at the core creating a highly negatively charged region.

At this point either deuterons or protons and B^{11} nuclei are injected into the cusped magnetic field. Because of their positive charge they accelerate towards the negative center. Most of them traverse the center toward the other side of the reactor. However, the negative charge of the electron ball pulls them back to the center. The process repeats itself thousands of times until the deuterons of the boron nuclei and protons collide with a large enough frequency to fuse together releasing energy in the process.

In the case of the pB^{11} reaction, the resulting 3 He^4 nuclei are deposited on an electrical grid forcing electrons to flow creating an electrical current. This direct energy conversion process is much more efficient than the thermal conversion process that would be used in the DT fusion cycle.

Inertial Electrostatic Fusion offers the following advantages:

1. The ability to construct small, compact power reactors that are 1-3 percent the size of current magnetic confinement reactors.
2. Clean, neutronless fusion cycles using initially the semi-catalyzed or the catalyzed DD reaction and eventually the pB^{11}fusion reaction.
3. With reactions producing primarily charged particles, direct energy conversion with high efficiency can be contemplated.
4. Fusion reactions with charged particles can be the basis of a fusion space propulsion system with high specific impulse I_{sp} [4].
5. Relatively simple engineering with commercial viability within 6-10 years.
6. Low cost per unit in the range of $150-200 million from program inception to demonstration of net power production.
7. The use of sustainable abundant fuel supplies as deuterium or boron in a pure fusion device, in addition to thorium in a hybrid fusion-fission device. Boron is one of the Earth's most common and elements occurring with a natural abundance of 80.1 a/0 B^{11} and 19.9 a/0 B^{10} in boron. It occurs in the Mojave Desert in California and is used in the production of flame retardants, eye drops and flat panel displays. Thorium is a byproduct of the production of the rare earth elements and is 4 times as abundant as uranium in the Earth's crust.

EXPERIENCE WITH CUSPED CONFIGURATIONS

A characteristic problem with the cusped configurations is that too many electrons escape from the system. The cause is that the magnetic field that created the electron ball at the center of the device also directed some electrons into the metallic walls of the electromagnetic coil containers and support structures. For viable cusped systems, the electron loss problems must be solved.

It is easier to work with DD fusion which requires 20 keV ions compared with pB^{11} fusion which requires ten times as much ion energy at 200 keV. Larger reactors would require larger high voltage power supplies, transformers and switches, as well as larger heat rejection and cooling systems.

It must be admitted that no closed-box machine can ever yield net fusion power. Open recirculating Magrid machines and systems are required. This is an immutable result of the

determination of losses of electrons in experiments, that show that losses to surfaces that are not magnetically shielded must be kept to less than 10^{-5} or so of the cusp axis flow of electrons in the WB effect at $\beta = 1$.

This is impossible for two reasons:

1. It is not practically possible to cover all but 10^{-5} of the entire surface of a box containing the interior plasma, with magnetic oils that protect all of this surface, and
2. Even if this were possible, it is not possible to protect against losses directly along the cusp axes to the end plates that bound each cusp. These intrinsic losses are inherent in the magnetic topology of a closed box system and forever prevent this from operating at small losses.

The inescapable conclusion is that all polyhedral Polywell machines must operate as open recirculating devices, and that all such systems must have essentially no B-field unshielded surface area available to electrons in the machine, itself. This means that all structure containing B field-generating coils must be conformal to the fields so produced, thus coil containers must have elliptical or circular cross-sections. If not, there will be large regions in which the B fields go into the metal surfaces at an angle rather than circulate around such surfaces. The electrons will simply drive along these intersecting B fields, directly into the metal, to yield excessive losses.

Because of this, it is also evident that – no matter their individual plan form shape (i.e. circles, squares, triangles, polygons etc.) – magnet coils must not touch at their adjacent corners, but must be spaced sufficiently far apart to ensure that no B fields intersect their containers. In this way, electrons can recirculate freely around all parts of each coil, and thus operate with minimal losses. These corner spacing line-like-cusps give local current flows that reduce the effective e- trapping factor (Gmj) in the machine interior from that for pure Wiffle Ball (WB) behavior alone. However, the reduction is not sufficient to prevent ready attainment of the e-density ratios inside/outside, required for avoidance of external arcing.

Operating as recirculating (Magrid) machines means that there will be an external region between the machine and its containing exterior wall, in which Paschen arc breakdown can occur, unless both external electron and neutral gas density can be kept below some critical level. To do so requires large scale vacuum pumping in this exterior region. However, this level is so low that it cannot produce significant fusion rates inside the machine, if the densities are allowed to be the same across the system. Thus, some means must be found to ensure large electron density within the machine, while maintaining it at small levels outside.

This requires that the ionization of neutral gas density within the machine be very large relative to that outside; and this can be attained only by neutral gas injection directly into the machine, followed by subsequent very rapid ionization of this gas, before it can escape into the exterior region. In small machines this is difficult, as time scales for neutral transport to the exterior are measured in fractions of a millisecond, and dimensions within the machines are not sufficient to allow rapid ionization at the limited electron currents and densities attainable. In large machines, such as power reactors, typically 2-3 m in diameter, with high power electron drives (e.g. 100-500 Amps at 15-30 kV for DD and 180-220 kV for pB^{11}), it is easy to show that almost total ionization of the inflowing neutral gas can be achieved in a few centimeters of electron path length at the system edge, but small devices cannot reach this condition.

Thus, in small systems there is a big incentive to attempt to fuel the machine with ions injected from ion guns placed on the cusp axes. This, however, poses the problem that the ion

guns must be at the machine voltage, thus constitute very visible and attractive potential sinks for the electrons, as they cannot be fully magnetically shielded, as can the magnets themselves. In this situation, it appears that the only way to test these principles in small machines is to try to use capacitor discharge drives, timed precisely so that the neutral gas injection is started with the cap drives, and the electron well drives are also started simultaneously. This requires very precise timing, which is difficult but has been achieved in such tests, however, this entire problem goes away in machine sizes for net power production. This conclusion echoes that of previous years. If it were possible to provide ion injection surfaces on the inside faces of the magnets (but no such sources exist), this might solve the problem in small test devices, however, ions injected at low energy at such positions will, themselves, be trapped in the magnet surface B fields, and have to cross into the potential well gradient by E x B drift forces, which may not be practicable. In reactor-size systems, ions formed within the interior field surface boundary will fall to the center naturally, under the effect of the high radial potential gradient that makes the deep well of the system.

Finally, in terms of practical limitations it was noted that the basic physics concept presumes magnet coils of near-zero physical cross-section, which touch at acute to right angles at the corners of the polyhedral-vertex boundaries on which they are supposed to lie. This has always given a “funny cusp” at such touching corners, which has been noted as having essentially zero tangential radius, although it also has zero B field. However, with realistic coils of finite dimensions (i.e. the coil cross-sections are a not insignificant fraction of the machine or coil major radius) this “funny cusp” expands to involve a rectangular region bounded by the dimensions/size of the coil containers. This rectangular region will have competing fields at 90 degree intervals, thus will act as an unshielded area for electron losses from the machine drive. The fractional size of this unshielded area is always found (from magnet design studies using real conductors) to be in the range of 0.01-0.1 of the total surface area of the coil containers. Since unshielded fractional areas above 10^{-5} to $10^{-}4$ are untenable, this effect gives losses that are ca. 1000x too large for useful fusion output.

The only way to avoid this, with coils of realistic finite size, using realistic conductors (e.g. superconductors) is to space the coils a distance from each other, as described in above, so that no B fields intersect the coil container metal surfaces, but rather the field lines flow in parallel between the spacing at these corners. To achieve the ideal polyhedral trapping effect with proper coil magnetic insulation, the coil centerlines may also be offset so as to appear directly along the edge vertices, although this is not an essential requirement. Thus, the only coil configuration that can work to best advantage is one in which the coils are contained in circular cross-section tubes, turning at each corner through a small straight section, which is spaced a distance away from its not quite-touching adjacent neighbor coil. Analysis shows that this spacing should be at least 3-8 gyro radii of the electrons in the coil surface field. This will avoid all direct incident electron impact but, as noted previously, will result in increased electron flow between inside and outside due to the fact that the spaced regions act like small line cusps rather than point cusps. Greater coil spacing can be used but only at the price of lesser internal trapping. A balance must be struck between Paschen arcing exterior density, and interior density required for the desired fusion output. Fortunately, it has been found that a margin of about 1,000 times is available in design for these conditions.

DISCUSSION

Large fusion machines do not suffer from the problems of compact machine to a significant degree, but they cost a great deal more. Costs tend to scale as the cube of the system size and the square of the B field. Thus, full-scale machines and their development will cost in the range of $180–200 million, depending on the fuel combination selected. These cost estimates closely reproduce those made throughout the USN program life, from its earliest work in 1991 to its conclusion in mid-2006 including those made at interim reviews in 1995 and 1999. USA Navy costs expended to date in this program have been approximately $18 million over about 10 years.

Compact machines with their low plasma amplification factors of Q_p around 0.01, can primarily be used as neutron sources for driving a future thorium fuel cycle. The nuclear performance of a fusion-fission hybrid reactor having a molten salt composed of Na-Th-F-Be as the blanket fertile material and operating with a catalyzed Deuterium-Deuterium (DD) plasma is compared to a system with a Li-Th-F-Be salt operating with a Deuterium-Tritium (DT) plasma. In a reactor with a 42-cm thick salt blanket followed by a 40-cm thick graphite reflector, the catalyzed DD system exhibits a fissile nuclide production rate of 0.88 Th(n,γ) reactions per fusion source neutron. The DT system, in addition to breeding tritium from lithium for the DT reaction yields 0.74 Th(n,γ) breeding reactions per fusion source neutron. Both approaches provide substantial energy amplification through the fusion-fission coupling process.

The use of Diode and Wiffle Ball (WB) cusped magnetic field configurations is discussed in the context of their use as compact drivers in Electrostatic and Electrodynamic Inertial Confinement (EIC) Fusion, for a Fusion-Fission Hybrid using a thorium molten salt breeder. The use of a fusion fission thorium hybrid in association with these configurations considering the catalyzed DD and the DT fusion reactions and a molten salt using Th^{232} as a U^{233} breeder is analyzed.

Energy and material balances in the coupled system is conducted. It shows that the energy multiplication in the coupled system approaches infinity as the conversion ratio of the fission satellites approaches unity.

Such a configuration would allow enough energy breakeven for a sustainable long term energy system with a practically unlimited fuel supply base. Deuterium can be extracted from water in the world oceans, and thorium is four times more abundant than uranium in the Earth's crust.

The approach would provide the possibility for the eventual introduction of aneutronic fusion cycles such as the pB11 cycle for energy production as well as for space propulsion.

Such an alternative sustainable paradigm would provide the possibility of an optimized fusion-fission thorium hybrid for long term fuel availability with the added advantages of higher temperatures thermal efficiency for process heat production for a future hydrogen economy,, proliferation resistance and minimized waste disposal characteristics.

REFERENCES

1. Magdi Ragheb, George Miley, James Stubbins and Chan Choi, "Alternate Approach to Inertial Confinement Fusion with Low Tritium Inventories and High Power Densities, Journal of Fusion Energy, Vol. 4, Number 5, pp. 339-351, October 1985.

2. S. Glasstone and R H. Lovberg, "Controlled Thermonuclear Reactions, an Introduction to Theory and Experiment," Robert E. Krieger Publishing Company, Huntington, New York, 1975.

3. Robert W. Bussard, “The Advent of Clean Nuclear Fusion: Superperformance Space Power and Propulsion,” 57th International Astronautical Congress, Valencia, Spain, October 2-6, 2006.
4. R. W. Bussard, “Some Physics Considerations of Magnetic Inertial-Electrostatic Confinement: A New Concept for Spherical Converging-Flow Fusion,” Fusion Technology, Vol. 19, March 1991.
5. M. M. H. Ragheb, R. T. Santoro, J. M. Barnes and M. J. Saltmarsh, “Nuclear Performance of Molten Salt Fusion-Fission Symbiotic Systems for Catalyzed Deuterium-Deuterium and Deuterium-Tritium Reactors,” Nuclear Technology, Vol. 48, pp. 216-232, May 1980.
6. P. Caldirola and H. Knoepfel, “ Physics of High Energy Density,” Academic Press, New York and London, 1971.
7. M. Ragheb, “Gamma Rays Interactions with Matter,” in: “Nuclear, Plasma and Radiation Science. Inventing the Future,” https://netfiles.uiuc.edu/mragheb/www, 2011.
8. I. Langmuir and K. B. Blodgett, “Currents Limited by Space Charge between Concentric Spheres,” Research laboratory, General Electric Company, Schenectady, New York, February 9, 1924.
9. Philo T. Farnsworth, “Electric Discharge Device for producing Interactions nbetween Nuclei,: USA patent no. 3,258,402, Jume 28, 1966.
10. R. L. Hirsch, “Inertial-Electrostatic Confinement of Ionized Fusion Gases,” J. Appl. Phys., Vol, 38, No. 11, p. 4522, October 1967.
11 George H. Miley, Yibin Gu DeMora, J. M. Stubbers, R. A. Hochberg, T. A. Nadler, J. H. Anderi, “Discharge Characteristics of the Spherical Inertial Electrostatic Confinement (IEC) Device,” Plasma Science, IEEE Transactions, pp. 733-739, August 1997.
12. Carl C. Dietrich, “Improving Particle Confinement in Inertial Electrostatic Fusion for Spacecraft Power and Propulsion,” Ph. D. Thesis, Department of Aeronautics and Astronautics, Massachusetts Institute of Technology, MIT, February 2007.
13. M. Ragheb, “Fusion Energy Concepts,” in: “Nuclear, Plasma and Radiation Science. Inventing the Future,” https://netfiles.uiuc.edu/mragheb/www, 2011.
14. http://www.mare.ee/indrek/octave